An Event-Triggered Energy-Efficient Wireless Structural Health Monitoring System for Impact Detection in Composite Airframes

Hailing Fu, *Member, IEEE,* Zahra Sharif Khodaei, and M. H. Ferri Aliabadi

***Abstract*—In this paper, a low-power high-response wireless structural health monitoring system (WSHMS) is designed, implemented and experimentally evaluated for impact detection in composite airframes. Due to the rare, random and transitory nature of impacts, an event-triggered mechanism is adopted for allowing the system to exhibit low power consumption when no impact occurs and high performance when triggered. System responsiveness, robustness and energy efficiency are considered and modelled. Based on system requirements and functions, several modules are proposed, including filtering, impact detecting, local processing and wireless communicating modules. The filtering module increases the system robustness by attenuating background vibration noises. The impact detection module monitors impact categories, and when the impact energy is above a certain threshold, it generates a trigger (wake-up) signal for the local processing module. The local processing module is required to be responsive to impact events, capable of processing multiple sensing inputs and energy-efficient when no impact occurs. The wireless module transmits the processed data to the host station for impact evaluation. The whole design was implemented on a printed circuit board (100 $\times$ 65 mm). The response time is around 12 μs with an average current consumption lower than 1 mA when the impact activity is lower than 0.1%. The system exhibits high robustness to ambient vibration noises and is also capable of accurately and responsively capturing multiple sensing input channels (up to 24 channels). This work presents a low-latency energy-aware WSHMS for impact detection of composite structures. It can be adapted to monitor of other rare, random and ephemeral events in many Internet of Things applications.**

***Index Terms*—Structural health monitoring, wireless sensor networks, energy-efficient, event-triggered, high-responsiveness.**

I. Introduction

IN THE ERA of the Internet of Things (IoT), a wide infrastructure network of "things" is envisioned to form a pervasive computing environment which allows things to sense ambient conditions, exchange data and make decisions intelligently and autonomously [1]. Structural health monitoring (SHM) of aircraft composite structures is one of the promising applications for the IoT in terms of improving the aircraft operation safety and reducing maintenance costs [2]. Nowadays, composite materials have been widely adopted in aerospace engineering due to their advanced material properties. For Boeing 787 and Airbus 350 XWB, composites take more than 50% by volume, and the percentage is still increasing [3].

The authors are with the Department of Aeronautics, Imperial College London, London, SW7 2AZ UK e-mail: h.fu14@imperial.ac.uk.

Manuscript received April 19, 20xx; revised August 26, 20xx.

However, for composites, various forms of damage, including indentation, de-lamination and fibre cracking, can be caused by low-velocity impacts, such as bird strikes, tool drops during manufacturing or maintenance, or debris during taking-off and landing [4]. Significant degradation of material properties can occur due to barely visible impact damage [5]. Different detection technologies, including optical methods, eddy-current, ultrasonic inspection, acoustic emission, vibration analysis, thermography, and Lamb waves, have been investigated extensively to evaluate impact damage [6]–[11].

In general, depending on use of transducers, SHM can be divided into two cases: active sensing and passive sensing. For active sensing, both actuators and sensors are necessary. The monitored structure is excited by one actuator, and the structural dynamics are recorded by several sensors. Based on the changes in the propagating signals, damage location and severity can be determined [12]. The number and location of the transducers on the monitored structure can be optimized to increase the detection accuracy while avoiding adding too much additional weight and costs [13], [14]. Active sensing has well-defined input excitations, in terms of signal type, frequency and amplitude. The inspection (actuating and sensing) cycles can also be controlled explicitly (e.g. 5 inspections per hour). However, this method requires the system to generate a specific actuating signal, which means a signal generation module is inevitable in hardware design. Power consumption and system complexity can be issues in practice.

For passive sensing, only sensors are required. These sensors continuously monitor the host status. Impact-induced acoustic or stress waves are recorded for impact location and evaluation [15]. Continuous monitoring allows the system to be aware of any impacts immediately, and the avoidance of the actuating function reduces the system complexity and power consumption. However, when impacts are rare, continuous operation unavoidably wastes energy. In addition, the unknown impact sources in terms of impactor shape, material, input force direction and velocity, etc. create difficulties for signal processing. In order to address these issues, researchers have developed many signal processing methodologies. Sharif-Khodaei *et al.* established a methodology using artificial neural networks (ANNs) to localize impacts on a composite stiffened panel subjected to a wide range of impact masses, velocities, and energies [16]. Morse *et al.* adopted Bayesian updating and the Kalman filter in an ANN to characterize impacts for different input energies in operational conditions [17]. Sensor number and location have also been considered and optimized

to increase detection reliability and probability [18], [19].

Compared to the development of signal processing algorithms for both active and passive sensing, the design and instrumentation of wireless structural health monitoring systems (WSHMS) are under-developed, especially for composite airframes. For most of the current studies, data acquisition of impacts is conducted in the laboratory conditions using high-performance signal generators and data acquisition systems without the consideration of power consumption and system adaptability. However, in aircraft applications, device compactness (weight and size) [20], system capability [21], [22], integrity under operational condition [23] as well as power consumption [24], [25], are all critical design constraints.

II. Related Work

Dutta *et al.* presented a wireless sensor network (WSN) platform for detecting exceptional events in a power-conscious manner [26]. System responsiveness, power consumption and large-scale operation were considered. Rusci *et al.* developed a fully programmable ultra-low power smart camera node for always-on visual monitoring system [27]. An event-driven computational model was exploited to allow the system to stay in the idle mode when no events occur, reducing the power consumption. Sutton *et al.* designed a wireless sensing system for monitoring acoustic emissions [28]. An event-driven approach was also adopted to increase energy efficiency. System modelling, circuit design and power dissipation were studied and evaluated. Li *et al.* designed a piezoelectric transducer-based distributed WSN for SHM of concrete structures [29]. Both active and passive sensing approaches were adopted to detect impacts and damage in a concrete structure. However, the detailed impact localization method and system power consumption were not investigated.

In terms of WSHMSs for composite structures in aerospace engineering, low-latency signal acquisition, sensing coverage, multiple input channels, robustness to ambient noises and also ultra-low power consumption are all critical constraints. Impacts generally happen randomly in a short time frame. WSHMSs, therefore, should be capable of capturing the transitory events with a high sampling frequency. Continuous monitoring using piezoelectric sensors is a solution, but it requires the acquisition system to operate actively all the time, which is power consuming. Event-triggered monitoring has low power consumption [30], but system response delay should be properly addressed to avoid losing many initial-stage impact data, as these data (including the time of arrival (ToA) and the amplitude of the first peak (AoFP)) are important for impact localization and evaluation [31], [32]. In addition, for composite structures, such as fuselage and wings, a large area must be monitored. Therefore, for WSHMSs, a large-area coverage capability with low system complexity is essential.

Yuan *et al.* developed a multi-response-based wireless sensor network (WSN) using a field-programmable gate array to realize the large-scale impact monitoring with system weight and complexity reduced significantly [33]. This system solved the problems of localization conflicts and mid-region localization by uniting multiple leaf nodes. More work related to this research can be found in [34], [35]. Similarly, Aranguren *et al.* developed a WSHMS using active sensing for aeronautical structures [36]. Up to 12 input channels are designed for sensing and actuating. However, the device dimensions and power consumption are the disadvantages of the proposed system. In order to improve energy efficiency, Zhang patented a trigger circuit for low-power SHM systems [37]. The event-triggered mechanism was presented, but the power consumption and the response time were not discussed, and these parameters are critical for detecting rare, random and transitory impacts.

In this paper, the design, implementation and experimental evaluation of a WSHMS for impact detection of composite airframes is presented. Design constraints, including system responsiveness, robustness, sensing capability and low-power operation, are considered in the design and modelling stage. Different modules are designed according to the system functions. An event-triggered method is proposed to reduce the power consumption when no impact occurs and to enhance the system performance when activated. The detailed design process is presented, and the system is implemented on a printed circuit board. From the experimental evaluation, low power consumption, high responsiveness, sensing capability and robustness have been realized.

III. Wireless Structural Health Monitoring System

The operational principle of the whole WSHMS is presented for impact detection and evaluation. Functions and design constraints are introduced and discussed. Fig. 1 illustrates the system configuration. A WSN is established by sensor nodes distributed on the whole aircraft. Each node is in charge of several piezoelectric sensors in a group to monitor potential impacts in a particular area confined by this group. Different network topologies can be adopted for the WSN, including tree, star and fully connected [38]. As the aim of this study is not for topology optimization, a tree topology is adopted.

In this WSN, wireless sensor nodes perform different roles, including a coordinator, routers and end devices. When impacts occur, the sensor node (either end devices or routers) covering the impact area records the impact-induced signals from piezoelectric sensors. The data are then pre-processed.

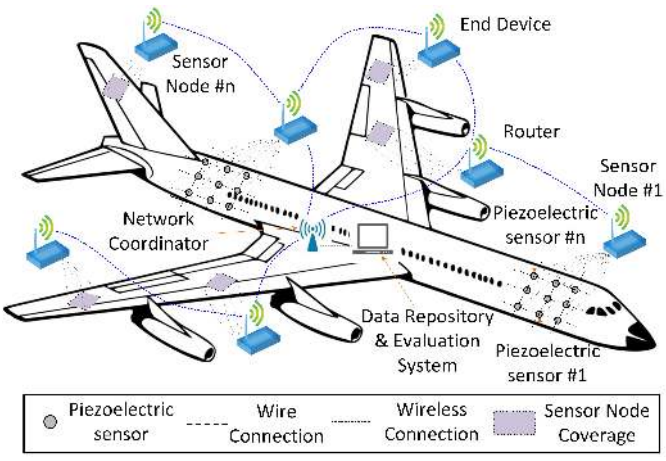

Fig. 1. Schematic of the WSHMS for impact detection and evaluation.

Selected features are extracted and wirelessly transmitted to the coordinator via routers. Post-processing is conducted in the host connected to the coordinator to evaluate impacts.

In the proposed WSHMS, the coordinator and routers are required to be active all the time in order to receive impact data immediately. These units are connected to the main power line; power consumption is not a major issue. However, end devices are normally powered by batteries or energy harvesters [39], [40] which have a limited discharging capability. In order to realize long-term operation and reduce maintenance costs, low-power consumption is the key. Therefore, energy efficiency is the first design constraint.

Impacts on an aircraft are rare, random and transitory. In order to capture these events, it is ideal for the sensing system to operate continuously. A high sampling frequency is also necessary to record these transitory events with sufficient accuracy. However, these requirements conflict with the design constraint of low-power operation. To overcome the above mentioned challenges, an event-triggered mechanism is necessary to allow the system to operate in the low-power mode when no events occur and to exhibit high performance and wireless communication capability when an impact happens. Another consideration for an event-triggered system is its responsiveness. In order to capture the whole profile of impact waves, especially the Time of Arrival (ToA), the system needs to be ready for recording as soon as it is triggered. Therefore, system responsiveness (low-latency) is the second design constraint.

For aircraft in operation, vibrations are abundant and distributed in a wide frequency range. These vibrations are also captured by piezoelectric sensors. False alarms may be generated due to local noises. In order to adapt the sensing system at run-time on board, filters and an appropriate triggering threshold are necessary to avoid recording false impacts which are not alarming for the structure. System robustness is, therefore, the third design constraint. In the following section, a WSHMS considering the constraints of low-power operation, system responsiveness and robustness is designed.

IV. Event-Triggered Energy-Efficient WSHMS

In this section, the detailed design and modelling of an event-triggered responsive low-power WSHMS is presented. The whole system is divided into several logical function blocks as shown in Fig. 2. Each function block corresponds to an event-triggered interface that is designed in Section V.

A. Operating Principle

As shown in Fig. 2, piezoelectric sensors are mounted on or embedded in composite plates to sense the stress waves, either from impacts or ambient vibrations. In order to avoid the noises caused by background vibrations, the event stream (data from piezoelectric sensors) first passes through a filtering module to reduce the noises. An appropriate filter needs to be designed to increase the signal-to-noise ratio. The filtered event stream is then compared to a pre-defined threshold V_d to determine if there is an impact or not. When an impact occurs, the trigger signal from the comparator output wakes up the local processor to record the signals from the data stream. Required parameters, such as ToA, are extracted from the data stream. The processor then wakes the wireless transmission module up, and those extracted parameters are wirelessly transmitted to the host for evaluating the impact. After that, the processor and the wireless transmission module turns into the low-power mode and wait for subsequent impact events.

B. System Modelling

An analytical model is established to study the responsiveness and average power consumption given the characteristics of impact events. It is assumed that the filter can eliminate all the noises from the environment. The impact events pass through the filter with an average arrival rate α. The arrival time of an impact i is denoted by t_i, where $t \in [0, \infty)$, and $i \in \mathbb{Z}$ is the corresponding impact order. A continuous random variable $\tau_d = t_{i+d} - t_i$ is defined to represent the time between impacts separated by an index difference $d \geqslant 1$. When $d = 1$, the variable τ_1 is the time interval between two successive impacts. Assuming that impacts happen independently and are distributed identically, the probability density function of τ_d can be given by the d-fold continuous convolution of f_{τ_k} (as given in Eq. (1)) using known properties of sums of continuous random variables [28], [41].

$$f_{\tau_d}(\tau) = (f_{\tau_k} * f_{\tau_{d-k}})(\tau) \text{ for } 1 \leq k \leq d-1 \tag{1}$$

The average arrival rate of impacts can be expressed as

$$\alpha = \frac{1}{\int_0^\infty \tau \cdot f_{\tau_1}(\tau) d\tau}. \tag{2}$$

For the trigger signal, the arrival rate β is determined by both the arrival rate α of impact event and the probability p_t of the impact signal to be regarded as an alarming impact which may cause damage in the composite materials. This probability p_t is determined by the threshold voltage V_d of the comparator module. When V_d is set very low, it means any detectable impacts from the piezoelectric sensors can trigger the system, and the probability p_t is close to 1, whereas when V_d is extremely high, p_t is significantly reduced (close to zero).

The impact-triggering events are modelled as independent Bernoulli trails, where the system is triggered with probability p_t, while the probability of not triggering the system is $1 - p_t$. The probability p_d of an impact have an index difference d can

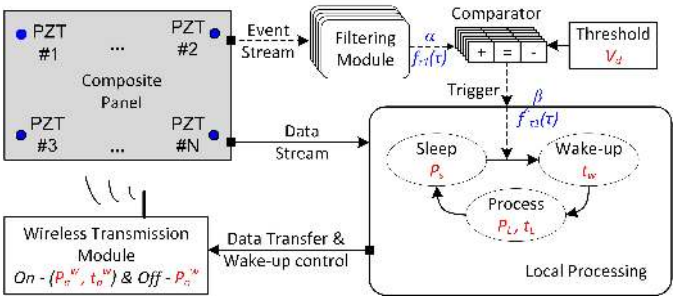

Fig. 2. Schematic of an event-triggered energy-aware wireless sensing system. The system is divided into several blocks according to the functions.

be expressed as the product of the probability of detecting an impact and the probability of $d-1$ of successive non-triggered impact events.

$$p_d = p_t \cdot (1 - p_t)^{d-1}. \tag{3}$$

The probability density function $\hat{f}_{\tau_1}(\tau)$ of the time interval of triggering events after the comparison module is given by

$$\hat{f}_{\tau_1}(\tau) = \sum_{d=1}^{\infty} p_d \cdot f_{\tau_d}(\tau). \tag{4}$$

Due to the exponential decay of p_d (as shown in Eq. (3)), the summation can be approximated by using a finite number of d. The average triggering arrival rate for the local processing module β can be expressed as the product of the impact arrival rate α and the triggering probability p_t, as expressed in Eq. (5).

$$\beta = p_t \cdot \alpha. \tag{5}$$

For the local processing module, it stays in the low-power mode with power consumption P_s when no trigger event occurs. Any trigger event can wake up this module in a time frame of t_w before the system can record and process the impact-induced voltage from piezoelectric sensors. In the processing state, this module extracts the necessary parameters from each input channel and sends these parameters to the wireless transmission module in a time frame of t_l. The average power consumption in the active process including wake-up and local processing is marked as P_l. After processing, this module turns into the low-power mode again and waits for the subsequent triggering events. The wireless module transmits the processed data to the host for impact evaluation. Its status is controlled by the local processing module. For the wireless module, the active power consumption and duration are noted as P_a^w and t_a^w, and P_o^w is for the low-power mode.

The responsiveness of the system is determined by the time spent in the wake-up stage, i.e. t_w. Short response time t_w is necessary to capture the transitory impacts. The energy consumption per impact is the total energy consumed by all the modules during both the low-power and active states. The total energy consumption per impact as a function of the time interval τ between successive impacts can be written as

$$\begin{aligned} u(\tau) = & \underbrace{P_l(t_w + t_l) + P_s(\tau - t_w - t_l)}_{\text{Local processing module}} \\ & + \underbrace{P_a^w t_a^w + P_o^w(\tau - t_a^w)}_{\text{Wireless module}} + \underbrace{P_{other} \cdot \tau}_{\text{Other modules}}, \end{aligned} \tag{6}$$

where P_{other} is the average power consumed by other modules, including the filtering and comparison modules.

According to the theory of the functions of continuous random variables [42], the probability density function $f_u(u)$ of the energy consumption per impact can be expressed as

$$f_u(u) = \frac{1}{P_s + P_o^w + P_{other}} \hat{f}_{\tau_1}(\tau). \tag{7}$$

The average power consumption of the whole system is then given as

$$P_{avg} = p_t \cdot \alpha \cdot \int_0^{\infty} u \cdot f_u(u) du \,/\, \tau. \tag{8}$$

Therefore, by knowing the statistical properties of the inputs (α, $f_{\tau_i}(\tau)$ and p_t) and operational parameters (V_d, P_l, P_s, t_w, t_l, P_a^w, t_a^w, P_o^w and P_{other}), the system performance, including the responsiveness t_w and the average power consumption P_{avg} can be determined and optimized.

C. Design Requirements

Based on the operational principle and modelling, the main system requirements can be generalized as: *Sleep as long as possible and wake-up immediately with high performance when triggered*. This will also be the design guideline for the hardware implementation. In the low-power (sleep) mode, the system power consumption ($P_s + P_o^w + P_{other}$) should be significantly reduced to maintain the average power consumption P_{avg} on a lower level. Passive circuit design is ideal for certain modules, such as the filter module and the comparator module, to satisfy the low-power constraint.

When alarming impacts occur, the system should response immediately to record impact data. The Lamb wave (stress wave in structures) propagation speed was measured in composite plates, and the values were in the range from 5 to 9 mm/μs in Ref. [43]. Therefore, the wake-up time t_w should be on the μs scale in order to capture the initial part of the impact data. The wake-up time t_w includes the response time of the comparator module and the start-up time for the local processor. Quick response is required for both modules.

Additional requirements, which are not critical but equally needed to be implemented, are summarized here. For the local processing module, high processing performance and multiple allowable sensing inputs are necessary. A high sampling rate is necessary to record the transitory impacts, and multiple inputs allow one end device to cover a larger monitoring area. For the filtering module, ambient vibration noises should be shielded with a suitable bandpass filter. A low-power mode and appropriate transmission distance are required for the wireless communication module. Device dimensions and weight should also be miniaturized, as these devices are designed for on-board equipment for condition-based maintenance.

V. System Design and Implementation

In this section, the design and implementation of the event-triggered energy-efficient WSHMS is discussed and presented. Interface circuits are designed according to the function blocks presented in Section III. Design constraints and requirements are considered as well.

A. High-pass Filter Interface

In order to minimize the influence of ambient vibration noises, a filter circuit is required. According to Radio Technical Commission for Aeronautics (RTCA) DO-160 Environmental Conditions and Test Procedures, the ambient vibration or testing conditions are normally below 2 kHz for a turbojet (and turbofan) [23], [44]. Therefore, the filter should be high-pass with a cut-off frequency of 2 kHz. Meanwhile, the filter circuit should have low-power consumption due to the demand of continuous operation. Therefore, a typical 2$^{\text{nd}}$ order passive

high-pass filter is designed, as shown in Fig. 3. This circuit can effectively eliminate the influence of vibration noises with no power supply. The governing equations for this circuit are

$$\begin{cases} j\omega C_1 \cdot (V_{in} - V_m) = V_{out}/R_1 + (V_m - V_{out}) \\ j\omega C_2 \cdot (V_m - V_{out}) = V_{out}/R_1. \end{cases} \quad (9)$$

When $C_1 = C_2 = C$ and $R_1 = R2 = R$, the amplitude attenuation G_a and phase shift θ can be expressed as

$$\begin{cases} G_a = \frac{V_{out}}{V_{in}} = \frac{1}{\sqrt{\left(1-\frac{1}{R^2C^2\omega^2}\right)^2 + \frac{9}{R^2C^2\omega^2}}} \\ \theta = \arctan\left(\frac{3}{\omega RC - \frac{1}{\omega RC}}\right). \end{cases} \quad (10)$$

Fig. 4 illustrates the design results of the filter interface with R = 2 MΩ and C = 100 pF. The cut-off frequency is 2.1 kHz, and based on the phase change curve, the filtered results are ahead of the original signal. This interface fulfils the function and requirement of filtering out the low-frequency vibration noises while requiring no power supply.

B. Comparator Module

For the comparator module, low power consumption and high responsiveness (short trigger latency) are critical for detecting impacts. This module is always-on to monitor potential impacts. Impact-induced voltages from different input channels (after the high-pass filter) are compared to a trigger threshold (V_d). This function can be implemented by op-amp comparators. Low response time and current dissipation are the main consideration for component selection. In this study, LM339A from Taxes Instruments is selected.

The design schematic of the comparator module is shown in Fig. 5(a). Each input channel (filtered signal) is connected to a comparator and compared with a threshold V_d which is generated by a voltage divider circuit as shown in Fig. 5(a),

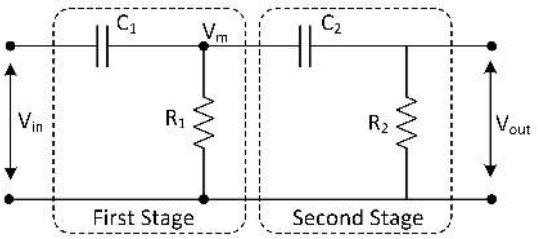

Fig. 3. Design of a typical 2nd order passive high-pass filter. Each input sensor channel needs an individual filter for noise shielding.

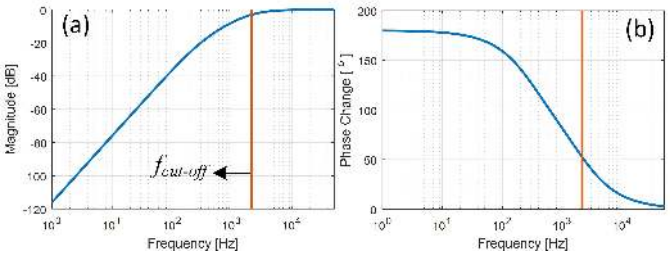

Fig. 4. Amplitude attenuation and phase change of the passive high-pass filter with R = 2 MΩ and C = 100 pF.

and the value is $V_d = V_{cc} \cdot R_2/(R_1 + R_2)$. By changing the ratio of R_1/R_2, the reference voltage can be modified, which means the detectable impacts can be adjusted. In addition, as the voltage divider consumes power, larger resistances are required for R_1 (= 7.4 MΩ) and R_2 (= 680 kΩ).

When there is no impact, the voltage outputs for all the channels are lower than V_d (or V_{Ref}). The output status $Out\ i$ (where i = 1, 2,..., n) for all the comparators are $open{-}circuit$, as defined by the comparator function. Therefore, the trigger signal V_{trg} is equal to V_{cc}. When one of the channels detects any impact events, the input voltage V_{Chi} (i = 1, 2,..., n) is larger than V_{Ref}. The output status for this comparator turns to $ground$. As a result, the trigger signal V_{trg} is grounded. The falling edge of the trigger signal V_{trg} can be used to wake up the subsequent local processing module.

The comparator module was implemented and tested on a breadboard. The experimental results are shown in Fig. 5(b). The threshold voltage V_d (V_{Ref}) is set as 0.25 V. For each input channel, a ±3 V and 0.5 Hz sine wave in a short duration (10 s) is applied at different instances, as shown in Fig. 5(b). The trigger signal is grounded whenever the input voltage from any channel is larger than the threshold. Otherwise, the trigger signal maintains high at 3 V. The duration for the falling edge was measured as 123 ns with a 1500 Ω pull-up resistance R_t.

The value of the pull-up resistor R_t needs to be carefully selected, as the resistor consumes power ($P_{trg} = V_{cc}^2/R_t$) when the trigger signal is grounded. Low power consumption can be achieved by a large resistance. However, the duration for the falling edge is also determined by the pull-up resistance and the internal capacitance (C_{in}) of the comparator. The time constant is $\tau_c = R_t \cdot C_{in}$. Therefore, lower resistance values are ideal to reduce the response time, but the low resistance also increases the power consumption P_{trg}. Fig. 5(c) illustrates the response time and active current consumed by R_t for different resistances. As the system responsiveness is more important, and the active current can be averaged by the extremely low active duration, the pull-up resistor is selected as 1 kΩ in this design. The quiescent current of the whole comparator module was measured to be 0.81 mA when no impact events occur.

C. Local Processing Module

The local processing module stays in the low-power mode for the most of the operational time and wakes up immediately when triggered. After waking up, this module records the voltage from each input channels using built-in analog-to-digital converters (ADCs). A high conversion speed (sampling rate) is necessary to record those transitory impacts. Based on the recorded data, necessary parameters, such as ToA, are extracted from each channel, and then transferred to the wireless transmission module. For ADCs, the available channels should be as many as possible in order to allow more piezoelectric sensors to be connected. In that case, a larger monitoring area can be covered by one sensing system. In summary, for this module, the requirements include quick wake-up response, multiple ADC channels, high conversion speed, and also available low-power modes.

Considering these requirements, a micro-controller (MCU) STM32L476ZE from STMicroelectronics is adopted to imple-

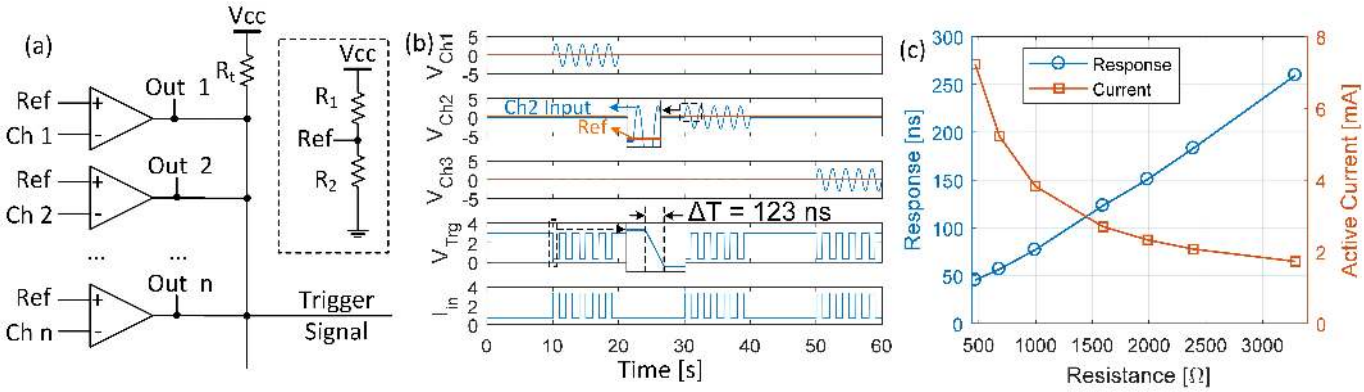

Fig. 5. Design and experimental results of the comparator module. (a) Design Schematic; (b) input voltages (unit: V) for different channels, output trigger signal (V) and system power consumption (mA); (c) response delay and active current for different pull-up resistances R_t. R_t was 1.5 kΩ for Fig. 5(b).

ment the local processing functions. This MCU is based on the high-performance ARM® Cortex®-M4 32-bit core operating at a frequency of up to 80 MHz. It has 24 ADC channels with the conversion speed up to 5.33 Msamples/s [45]. It has seven different low-power operation modes, including sleep, stop, standby and shut-down mode.

For the low-power operation, the power consumption P_s for the low power mode, and the wake-up time t_w are critical for the overall performance. Table I summarizes the low-power modes and their operational characteristics for this MCU. Stop 1 and Stop 2 present a good balance between the current consumption and wake-up time.

TABLE I
LOW-POWER MODES AND THEIR OPERATIONAL CHARACTERISTICS [45].

Low-power mode	Current consumption	Wake-up time
Sleep	13 - 37 µA/MHz	6 cycles
Stop 0	108 µA	0.7 µs in SRAM 4.5 µs in Flash
Stop 1	6.6 µA w/o RTC 6.9 µA RTC[a]	4 µs in SRAM 6 µs in Flash
Stop 2	1.1 µA w/o RTC 1.4 µA RTC	5 µs in SRAM 7 µs in Flash
Standby	0.12 µA w/o RTC 0.42 µA RTC	14 µs
Shut-down	0.03 µA w/o RTC 0.33 µA RTC	256 µs

[a] RTC is the abbreviation of real-time clock.

D. Wireless Transmission Module

The wireless transmission module is employed to transmit the processed data to the host station for impact evaluation. The considerations for this module is the transmission distance and also power consumption. As the data has been pre-processed by the local processing module, the amount of data required to be transmitted is marginal. Therefore, signal transmission latency and transmission rate are not the priority. For wireless communication, ZigBee, Bluetooth Low Energy and Wi-Fi are also possible options. ZigBee is adopted in this research due to its versatile network topologies [46].

In this study, the wireless communication module "Digi XBee® Zigbee" is adopted. This module has a communication range of 60 m for indoor (urban) conditions and 1200 m for outdoor (RF Line-of-sight) conditions [47]. The transmit power is 3.1 mW (+5 dBm) / 6.3 mW (+8 dBm). This module can be controlled to stay in a low-power sleep mode or the active mode by asserting or de-asserting the On/Sleep pin. This control is realized by the local processing module.

The operational principle of the wireless module in the whole network is depicted in Fig. 6. This module is in the sleep mode when no data transmission is required, and is woken up by the MCU when impact data is processed and ready

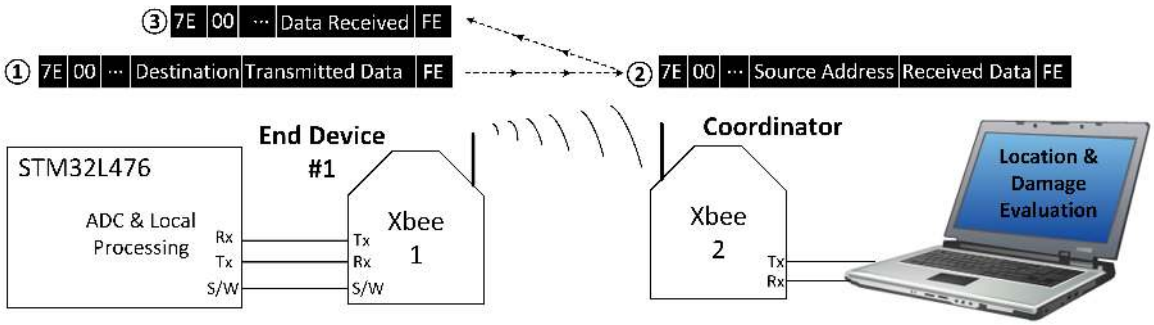

Fig. 6. Operation Principle of the wireless transmission module. The Sleep/On status is controlled by the MCU using the S/W pin. Detected data is transmitted wirelessly to the coordinator connected with the host station. ①: transmitted package; ②: received package and ③: acknowledgement package.

to be transmitted. The end device sends a data package ① containing the impact information to the coordinator using the Application Programming Interface (API) mode. Information, including package type, destination address and impact data, is included in Package ①. After the coordinator receives this impact information Package ②, the coordinator saves the received impact data and sends an acknowledgement package ③ to the end device. Then, the end device enters the sleep mode to save energy. Based on the extracted impact data received in Package ②, the impact can be evaluated by the host station, where the coordinator is located. The data length of an impact data ① from a sensor node with n sensors is $(2n+14)$ bytes, if two parameters (ToA and AoFP) with 8-bit resolution are extracted from each sensor data set.

E. System Integration and Implementation

Based on the above discussion, the whole system is integrated and implemented on a printed circuit board (PCB), as shown in Fig. 7. The overall dimensions are 100 × 65 mm. This PCB is divided into six blocks according to its functions. 12 input channels (the channel number can be extended up to 24) are designed with their own high-pass filters and bridge rectifiers. Bridge rectifiers are introduced due to the fact that this MCU only accepts positive input voltages. The rectified voltages V_i^r (i = 1, 2, ..., 12) are compared with the threshold voltage in the event monitoring circuit (comparator).

The trigger signal is connected to the MCU to wake it up when an impact occurs. The rectified voltages V_i^r also connect to 12 ADC channels on the MCU. After waking up, this MCU records all the inputs and extracts selected features, such as ToA, from these input signals. The MCU is also associated with the wireless transmission module (ZigBee Module) which is used for data communication. The On/Sleep state of this module is controlled by the MCU.

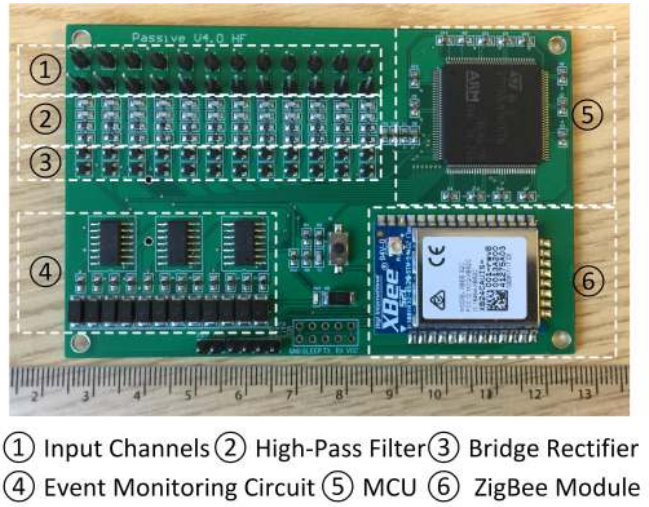

Fig. 7. Implementation of the event-triggered energy-efficient wireless sensing system for impact detection and localization. The whole system is divided into six blocks according to the functions.

VI. System Evaluation and Discussion

This section presents the evaluation and discussion of system responsiveness, power consumption, robustness to background noises and also multiple-channel sensing capability.

A. Responsiveness

The low-power mode for the MCU is configured as Stop 1. The pull-up resistor R_t is 1 kΩ. The system responsiveness was measured by connecting one input channel to a piezoelectric sensor on a composite plate. The result for the system responsiveness is illustrated in Fig. 8. The impact event was recorded simultaneously by an oscilloscope as well to capture the whole waveform and to provide a reference for the ADC result. Fig. 8(a) is the rectified voltage from the piezoelectric sensor recorded by the oscilloscope at 2 Msps.

When the rectified voltage is larger than the trigger threshold, the comparator output turns to 0 V from 3 V, as shown in Fig. 8(b). The response time for the comparator output is noted as t_c which is 3.1 µs. The value is much larger than the results shown in Fig. 5(c). This can be explained by the ripples from the comparator output as shown in the expanded view (on the right side) in Fig. 8(b). These ripples are caused by the piezoelectric sensor output variation above or below the threshold during this short time frame.

The falling edge of the trigger signal wakes the MCU up, and the ADC recording process starts immediately. The wake-up time for the MCU t_m is 9.3 µs. This includes the initiation and stabilization time for ADC as well. Therefore, the total wake-up time t_w is 12.4 µs $(t_c + t_m)$. The initial impact data is lost due to the wake-up delay, as shown in Fig. 8(e). This is detrimental for extracting ToA. Strategies to overcome this issue will be discussed later.

Afterwards, ADCs take around 3 ms to record the impact data. Then the local processing function is enabled for 5.5 ms to extract the required information. When the data are ready, the wireless module is woken-up by the MCU for t_a^w = 1 ms. After receiving the acknowledge package from the host (showing the data has been received successfully by the coordinator), the wireless module is turned off by the MCU, and the MCU enters the low-power (Stop 1) mode as well.

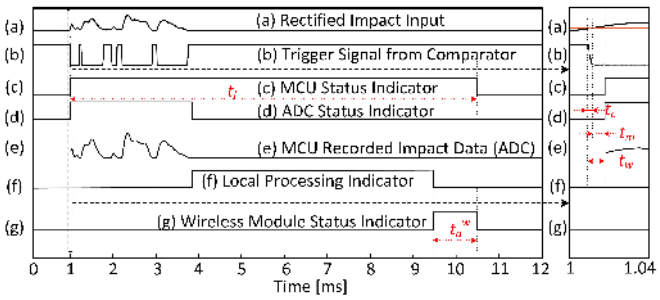

Fig. 8. Responsiveness of the wireless sensing system. The filtered impact input was measured using an oscilloscope at the same location as the MCU. Fig. 8(e) is the data recorded by the MCU at 220 kHz.

B. Power Consumption

As this wireless sensing system is designed to be powered by batteries or potential energy harvesters, system lifetime is also a big consideration. Low power consumption is ideal for the long-term operation. Here, the power consumption of the whole system is evaluated, as shown in Table II.

For the filter and bridge rectifier circuits, no power supply is required, as they are passive, and they operate continuously all the time. For the low-power mode, the comparator module consumes the highest current (0.81 mA for one comparator unit with 4 input channels). This value can be further reduced by adopting other low-power comparators, such as TS881 from STMicroelectronics [48], but the response time should be considered as well. As shown in Table II, the active power consumption for the MCU and ZigBee module is extensive. However, considering the rare, transitory nature of impact events, the average power consumption can be reduced to a moderate level because of the event-triggering mechanism.

Using the theory established in Section IV-B and considering different percentages of impact events in time, the system average power consumption and battery lifetime are compared to an always-on monitoring system, as shown in Fig. 9. To achieve a fair comparison, the ZigBee module for the always-on system is also considered to have two states, namely sleep and active. This module is active only when data is ready for transmitting, and enters the sleep module when transmission is completed.

According to Fig. 9, the low-power sensing system has much lower current consumption when the impact activity is low. Consequently, the battery lifetime is extended significantly. For example, when the impact activity is 0.1%, the average current (0.99 mA) for the low-power system is 12 times lower than that (11.7 mA) of an always-on system, and the lifetime is extended from 341 hours to 4034 hours.

Also, when the impact activity is low, which is the typical situation for impacts on aircraft, the average current consumption (0.99 mA @ 0.1% impact activity) for the low-power system is close to the current consumption level (0.98 mA) in the low-power mode. Two solutions are proposed here to further extend the system lifetime.

(1) Decrease the low-power mode current consumption. As shown in Table II, the comparator is the most current consuming module. Reducing the current requirement while maintaining the system response is one solution.
(2) Use energy harvesting technology. As there are abundant passive energy sources in the environment where the sensing systems mounted [49], [50], converting these energy sources into electricity to power the system can potentially allow the system to be fully autonomous.

TABLE II
POWER CONSUMPTION OF EACH MODULE FOR DIFFERENT MODES.

Module	Low-Power	Active	Active Duration
Filter	-	-	Always
Rectifier	-	-	Always
Comparator	0.81 mA[a]	3.83 mA	3 ms/impact[b]
MCU	0.07 mA	7.8 mA	10.5 ms/impact
ZigBee	0.10 mA	10.1 mA	1 ms/impact
Sum	0.98 mA	21.63 mA	10.5 ms/impact[c]

[a] One comparator unit with 4 input channels is considered.
[b] The active time is determined by the duration of impacts; 3 ms is believed to be an appropriate estimation.
[c] This is the total active time for the whole system; not all the modules are active for the whole period.

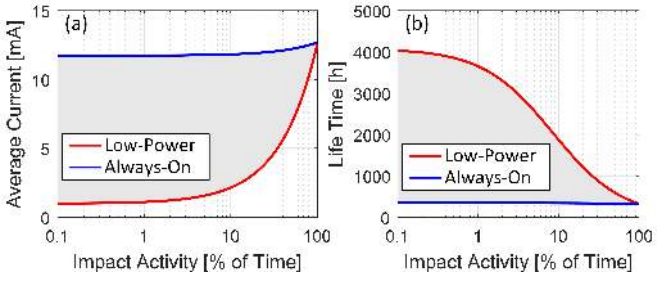

Fig. 9. Comparison of average current consumption (a) and battery lifetime (b) between a low-power system and an always-on system. The battery capacity (4000 mAh) is estimated based on the capability of two AA batteries.

C. System Robustness

For the monitoring system, it should not only be sensitive to all the alarming impacts, but also be able to avoid ambient vibration interruptions. The performance of the whole system was tested under vibration load levels representing aircraft operational environment, and the results are illustrated in Fig. 10. Ambient vibrations were generated by a closed-loop vibration set-up consisting of a TMS 2110E shaker and a 2050E09-FS power amplifier. A composite plate with a piezoelectric sensor was mounted on the shaker. The vibration frequency varied from 10 Hz to 700 Hz.

As shown in Fig. 10(a), the recorded vibration amplitudes of noises can be as high as 1 V. If the filter module is not applied, the local processing module can be easily woken up by ambient vibrations (Trigger threshold V_d = 0.25 V), even though no impact has occurred. As a result, false alarms and unnecessary power consumption can be arisen.

By applying the filter module, low-frequency noises from vibration can be removed effectively, as shown in Fig. 10(b). The whole system stays in the low-power mode although the noise amplitude is larger than the trigger threshold, as indicated in Fig. 10(c). This filter circuit also allows the impact detection module to adopt a low trigger threshold V_d because of the avoidance of low-frequency vibration interference. The low trigger threshold is beneficial to detect low-energy impacts and to wake up the processing module earlier to record the impact for a longer time window, especially at the initial stage.

The output voltage amplitude (<1.5 V) of impacts after filtering and rectification is much lower than the original signal (around 5 V) from the piezoelectric sensor, as shown in Fig. 10(a) and (b). The reason is discussed here. For impact-induced voltage, it has versatile frequency components (from low to high) due to the numerous vibration modes of Lamb waves [51]. The filter module also removes some low frequency components (below the cut-off frequency) from the impact signal. However, the high frequency components still

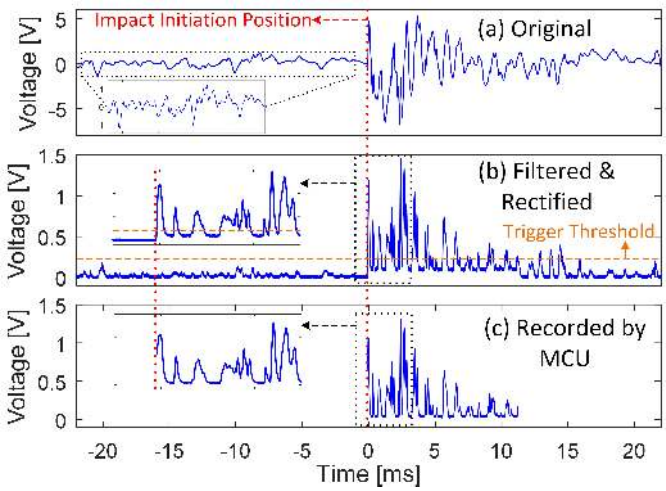

Fig. 10. Results of system robustness to ambient vibration noises. (a) Original signal from a piezoelectric sensor; (b) filtered and rectified signal measured by an oscilloscope and (c) data recorded by the local processing module. An impact was introduced at 0 s, as indicated by the red dotted line.

remain without the interference of background noises. These components can be used for impact detection and evaluation.

Fig. 10(c) is the signal recorded by the local processing module. The signal is the almost the same as the filtered and rectified voltage (Fig. 10(b)) recorded by an oscilloscope. Noises from ambient vibrations have been eliminated. Some data at the initial stage is lost due to the wake-up delay of the processor from a stop mode. Solutions for this issue will be discussed in the following sub-section.

D. Multiple Channel Performance

For impact detection and evaluation, multiple piezoelectric sensors in a group are necessary to localize impacts and to estimate the severity. Fig. 11 shows a typical sensor configuration for impact detection on a composite plate (290 × 200 × 4 mm). Eight sensors are mounted at the edges of the plate. Impacts occurring in the confined area of these sensors can be located and evaluated based on the data from each sensor.

Fig. 12 illustrates the sensing results from four piezoelectric sensors, including Sensor 1, 2, 3 and 4 in Fig 11. An impact was introduced to trigger the system and to test the multiple-channel performance. The impact location is marked on Fig. 11. The impact signal first arrived at Sensor 1 and triggered the system. Four channels were recorded simultaneously. All the initial stage signals were successfully captured apart from Sensor 1 (Ch 1 in Fig. 12).

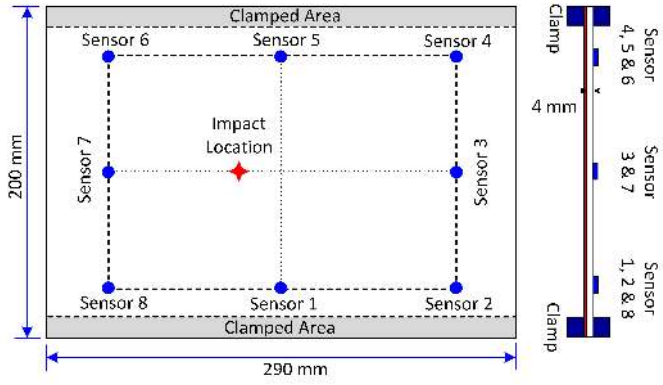

Fig. 11. Schematic of the composite plate showing the structural dimensions, impact locations and sensor installation locations.

Therefore, the potential impact detection and evaluation strategy is using one channel (closest to the impact location) as the trigger channel and the rest for sensing. As the waveforms for the rest channels are complete, all the necessary information, including the Time of Arrival (t_2, t_3 and t_4) and the amplitude of the first peak (P_2, P_3 and P_4), can be extracted for impact localization and evaluation. The sensor configurations and the number of sensing channels can be optimized to achieve the best sensing performance.

In some cases, sensors are equally distributed, when the impacts happens in the central area, the arrival time for different channels has marginal differences. Therefore, some sensing channels could also lose some critical initial-stage impact data. Comparing Fig. 13(b) to Fig. 13(a), the initial-stage data is lost in the data recorded by the local processing module. This lost data are necessary to determine the ToA information for impact localization. In order to recover the initial data, a simple but efficient moving-average method is implemented in the local processing module. The logical process of this method is

(1) Fill the lost data section with zeros;
(2) Calculate the mean value over a sliding window of length k across neighbouring elements of each point.

The recovery process is conducted by the local processing module automatically when the first detected point of the impact data is larger than a pre-defined threshold (e.g. 3% of the amplitude of the first peak). A certain number of zeros n_w (e.g. 100 points) are added at the beginning of the dataset for the purpose of conducting the moving-average algorithm. This number n_w is determined by the system wake-up delay

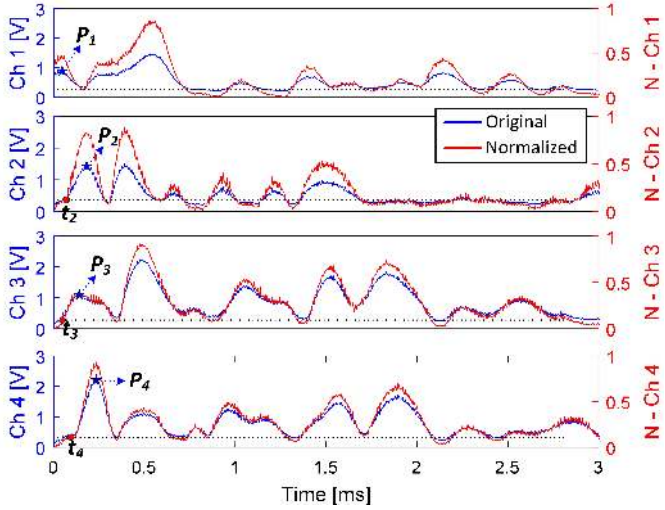

Fig. 12. Recorded and normalized data from four sensors. Ch i (i = 1, 2, 3, 4) corresponds to Sensor i (i = 1, 2, 3, 4) in Fig. 11. All the recorded data was divided by the maximum value from each channel to normalize the data. The first time to reach 0.1 in the normalized data is defined as the ToA.

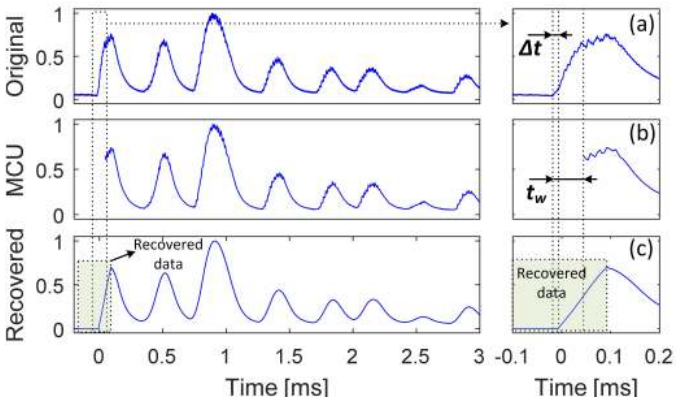

Fig. 13. Data recovery strategy for the initial-stage impact data. (a) Normalized original sensing data recorded by an oscilloscope, (b) normalized data recorded by the local processing module and (c) recovered data with the estimated initial-stage data.

t_w and the system sampling frequency f_s. The relationship can be defined as:

$$n_w = \alpha_0 \cdot t_w \cdot f_s, \tag{11}$$

where α_0 is the redundancy rate and $\alpha_0 > 1$.

The moving-average algorithm calculates the mean value of adjacent points over a sliding window of length k. The first time that the mean value exceeds the pre-defined threshold is defined as the Time of Arrival (ToA). The window length k can be automatically computed based on the sampling frequency f_s and the concerned impact signal frequency f_{im}. The relationship can be defined as:

$$k = \beta_0 \cdot f_s / f_{im}, \tag{12}$$

where β_0 is the window length coefficient. The window length cannot be too large; otherwise the signal features will be averaged out. Given that the sampling frequency is 220 kHz and the main signal frequency is around 2.5 kHz, $\beta_0 = 0.1$ and $k = 9$ are used to obtain enough window length for averaging while maintaining the impact signal features.

This method can be easily implemented in the local processing module without adding too much calculation complexity to the MCU. According to the result in Fig. 13(c), the recovered data has a close match to the original data. Hence, this method, which has a low calculation demand and tolerable accuracy can be applied to sensing channels, in which the initial-stage impact data are lost. In addition, this moving-average method also smooths the recorded data by the ADCs. This smoothed data is ideal for the local processing module to extract parameters, such as ToA and AoFP.

VII. Conclusion

In this paper, an innovative low-power high-response WSHMS is designed, implemented and evaluated for impact detection of composite airframes. In order to effectively monitor the rare, random and transitory impacts on aircraft structures, an event-triggered mechanism is adopted for the system to exhibit low power consumption when no impact occurs and high performance when triggered. System responsiveness, robustness and energy efficiency are considered and modelled. Based on the system requirements and functions, several modules are proposed, including filtering, impact detection, local processing and wireless communicating modules.

The filtering module increases the system robustness by eliminating ambient low-frequency vibrations. The impact detecting module monitors impacts above a pre-defined threshold which could be alarming to the structure and generates trigger (wake-up) signals for the local processing module when alarming impacts occur. The local processing module is required to be responsive to impact events, capable of processing multiple impact inputs and energy-efficient when no impact occurs. The wireless module transmits the processed impact data to the host station for impact detection and evaluation.

The whole design was implemented on a printed circuit board with the dimensions of 100 $\times$ 65 mm. The system response time for impact is around 12 µs with an average current consumption lower than 1 mA when the impact activity is lower than 0.1%. The system exhibits strong robustness to ambient vibration and also is also capable of accurately and responsively capturing multiple sensing input channels (up to 24 channels). An efficient and simple data recovering method using moving-average is proposed to address the issues of the missed initial-stage impact data due to the wake-up delay.

Acknowledgment

The research leading to these results has gratefully received partial funding from the European JTI-CleanSky2 program under the Grant Agreement n° 314768 (SHERLOC).

References

[1] J. Gubbi, R. Buyya, S. Marusic, and M. Palaniswami, "Internet of things (iot): A vision, architectural elements, and future directions," *Future generation computer systems*, vol. 29, no. 7, pp. 1645–1660, 2013.

[2] C. A. Tokognon, B. Gao, G. Y. Tian, and Y. Yan, "Structural health monitoring framework based on internet of things: A survey," *IEEE Internet of Things Journal*, vol. 4, no. 3, pp. 619–635, June 2017.

[3] R. Di Sante, "Fibre optic sensors for structural health monitoring of aircraft composite structures: Recent advances and applications," *Sensors*, vol. 15, no. 8, pp. 18 666–18 713, 2015.

[4] W. Staszewski, S. Mahzan, and R. Traynor, "Health monitoring of aerospace composite structures–active and passive approach," *composites Science and Technology*, vol. 69, no. 11-12, pp. 1678–1685, 2009.

[5] A. S. Nobari and M. H. F. Aliabadi, *Vibration-Based Techniques for Damage Detection and Localization in Engineering Structures*. World Scientific, 2018, vol. 10.

[6] M. H. F. Aliabadi and Z. Sharif Khodaei, *Structural Health Monitoring For Advanced Composite Structures*. World Scientific, 2017, vol. 8.

[7] M. Ghajari, Z. Sharif-Khodaei, M. Aliabadi, and A. Apicella, "Identification of impact force for smart composite stiffened panels," *Smart Materials and Structures*, vol. 22, no. 8, p. 085014, 2013.

[8] M. Salmanpour, Z. Sharif Khodaei, and M. Aliabadi, "Guided wave temperature correction methods in structural health monitoring," *Journal of Intelligent Material Systems and Structures*, vol. 28, no. 5, pp. 604–618, 2017.

[9] M. S. Salmanpour, Z. S. Khodaei, and M. H. Aliabadi, "Instantaneous baseline damage localization using sensor mapping," *IEEE Sensors Journal*, vol. 17, no. 2, pp. 295–301, 2017.

[10] M. S. Salmanpour, Z. Sharif Khodaei, and M. Aliabadi, "Impact damage localisation with piezoelectric sensors under operational and environmental conditions," *Sensors*, vol. 17, no. 5, p. 1178, 2017.

[11] Z. Sharif Khodaei and M. Aliabadi, "A multi-level decision fusion strategy for condition based maintenance of composite structures," *Materials*, vol. 9, no. 9, p. 790, 2016.

[12] J.-B. Ihn and F.-K. Chang, "Pitch-catch active sensing methods in structural health monitoring for aircraft structures," *Structural Health Monitoring*, vol. 7, no. 1, pp. 5–19, 2008.

[13] M. Salmanpour, Z. Sharif Khodaei, and M. Aliabadi, "Transducer placement optimisation scheme for a delay and sum damage detection algorithm," *Structural Control and Health Monitoring*, vol. 24, no. 4, 2017.

[14] M. Thiene, Z. S. Khodaei, and M. Aliabadi, "Optimal sensor placement for maximum area coverage (mac) for damage localization in composite structures," *Smart materials and structures*, vol. 25, no. 9, p. 095037, 2016.

[15] H. K. Jung and G. Park, "Integrating passive-and active-sensing techniques using an l-shaped sensor array for impact and damage localization," *Journal of Intelligent Material Systems and Structures*, p. 1045389X17733059, 2017.

[16] Z. Sharif-Khodaei, M. Ghajari, and M. Aliabadi, "Determination of impact location on composite stiffened panels," *Smart Materials and Structures*, vol. 21, no. 10, p. 105026, 2012.

[17] L. Morse, Z. S. Khodaei, and M. Aliabadi, "Reliability based impact localization in composite panels using bayesian updating and the kalman filter," *Mechanical Systems and Signal Processing*, vol. 99, pp. 107–128, 2018.

[18] V. Mallardo, M. Aliabadi, and Z. S. Khodaei, "Optimal sensor positioning for impact localization in smart composite panels," *Journal of intelligent material systems and structures*, vol. 24, no. 5, pp. 559–573, 2013.

[19] V. Mallardo, Z. Sharif Khodaei, and F. M. Aliabadi, "A bayesian approach for sensor optimisation in impact identification," *Materials*, vol. 9, no. 11, p. 946, 2016.

[20] H. Bai, M. Atiquzzaman, and D. Lilja, "Wireless sensor network for aircraft health monitoring," in *Broadband Networks, 2004. BroadNets 2004. Proceedings. First International Conference on*. IEEE, 2004, pp. 748–750.

[21] F. Sutton, R. Da Forno, J. Beutel, and L. Thiele, "Blitz: A network architecture for low latency and energy-efficient event-triggered wireless communication," in *Proceedings of the 4th ACM Workshop on Hot Topics in Wireless*. ACM, 2017, pp. 55–59.

[22] J. Jiang and C. Claudel, "A high performance, low power computational platform for complex sensing operations in smart cities," *HardwareX*, vol. 1, pp. 22–37, 2017.

[23] M. S. Salmanpour, Z. Sharif Khodaei, and M. H. Aliabadi, "Airborne transducer integrity under operational environment for structural health monitoring," *Sensors*, vol. 16, no. 12, p. 2110, 2016.

[24] A. B. Noel, A. Abdaoui, T. Elfouly, M. H. Ahmed, A. Badawy, and M. S. Shehata, "Structural health monitoring using wireless sensor networks: A comprehensive survey," *IEEE Communications Surveys & Tutorials*, vol. 19, no. 3, pp. 1403–1423, 2017.

[25] Y. Lee, D. Blaauw, and D. Sylvester, "Ultralow power circuit design for wireless sensor nodes for structural health monitoring," *Proceedings of the IEEE*, vol. 104, no. 8, pp. 1529–1546, 2016.

[26] P. Dutta, M. Grimmer, A. Arora, S. Bibyk, and D. Culler, "Design of a wireless sensor network platform for detecting rare, random, and ephemeral events," in *Proceedings of the 4th international symposium on Information processing in sensor networks*. IEEE Press, 2005, p. 70.

[27] M. Rusci, D. Rossi, E. Farella, and L. Benini, "A sub-mw iot-endnode for always-on visual monitoring and smart triggering," *IEEE Internet of Things Journal*, vol. 4, no. 5, pp. 1284–1295, 2017.

[28] F. Sutton, R. Da Forno, D. Gschwend, T. Gsell, R. Lim, J. Beutel, and L. Thiele, "The design of a responsive and energy-efficient event-triggered wireless sensing system," *Proc. of ACM EWSN*, pp. 144–155, 2017.

[29] P. Li, C. Olmi, and G. Song, "Energy efficient wireless sensor network for structural health monitoring using distributed embedded piezoelectric transducers," in *Sensors and Smart Structures Technologies for Civil, Mechanical, and Aerospace Systems 2010*, vol. 7647. International Society for Optics and Photonics, 2010, p. 764715.

[30] K. D. Champaigne, "Low-power electronics for distributed impact detection and piezoelectric sensor applications," in *Aerospace Conference, 2007 IEEE*. IEEE, 2007, pp. 1–8.

[31] T. Clarke and P. Cawley, "Enhancing the defect localization capability of a guided wave shm system applied to a complex structure," *Structural Health Monitoring*, vol. 10, no. 3, pp. 247–259, 2011.

[32] J. P. McCrory, S. K. Al-Jumaili, D. Crivelli, M. R. Pearson, M. J. Eaton, C. A. Featherston, M. Guagliano, K. M. Holford, and R. Pullin, "Damage classification in carbon fibre composites using acoustic emission: A comparison of three techniques," *Composites Part B: Engineering*, vol. 68, pp. 424–430, 2015.

[33] S. Yuan, Y. Ren, L. Qiu, and H. Mei, "A multi-response-based wireless impact monitoring network for aircraft composite structures," *IEEE Transactions on Industrial Electronics*, vol. 63, no. 12, pp. 7712–7722, 2016.

[34] L. Qiu, S. Yuan, P. Liu, and W. Qian, "Design of an all-digital impact monitoring system for large-scale composite structures," *IEEE Transactions on Instrumentation and Measurement*, vol. 62, no. 7, pp. 1990–2002, 2013.

[35] S. Yuan, H. Mei, L. Qiu, and Y. Ren, "On a digital wireless impact-monitoring network for large-scale composite structures," *Smart Materials and Structures*, vol. 23, no. 8, p. 085007, 2014.

[36] G. Aranguren, P. Monje, V. Cokonaj, E. Barrera, and M. Ruiz, "Ultrasonic wave-based structural health monitoring embedded instrument," *Review of Scientific Instruments*, vol. 84, no. 12, p. 125106, 2013.

[37] C. Zhang, "Trigger circuit for low-power structural health monitoring system," Mar. 19 2013, uS Patent 8,401,804.

[38] G. Han, L. Liu, J. Jiang, L. Shu, and G. Hancke, "Analysis of energy-efficient connected target coverage algorithms for industrial wireless sensor networks," *IEEE Transactions on Industrial Informatics*, vol. 13, no. 1, pp. 135–143, 2017.

[39] H. Jiang, M. E. Kiziroglou, D. C. Yates, and E. M. Yeatman, "A motion-powered piezoelectric pulse generator for wireless sensing via fm transmission," *IEEE Internet of Things Journal*, vol. 2, no. 1, pp. 5–13, 2015.

[40] H. Fu and E. M. Yeatman, "A methodology for low-speed broadband rotational energy harvesting using piezoelectric transduction and frequency up-conversion," *Energy*, vol. 125, pp. 152–161, 2017.

[41] C. M. Grinstead and J. L. Snell, *Introduction to probability*. American Mathematical Soc., 2012.

[42] A. Papoulis and S. U. Pillai, *Probability, random variables, and stochastic processes*. Tata McGraw-Hill Education, 2002.

[43] R. Badcock and E. Birt, "The use of 0-3 piezocomposite embedded lamb wave sensors for detection of damage in advanced fibre composites," *Smart Materials and Structures*, vol. 9, no. 3, p. 291, 2000.

[44] "DO-160C Environmental Conditions and Test Procedures for Airborne Equipment," Radio Technical Commission for Aeronautics (RTCA): Washington, Tech. Rep., 1989.

[45] (2018) Stm32l476ze. [Online]. Available: http://www.st.com/zh/microcontrollers/stm32l476ze.html

[46] K. Shahzad and B. Oelmann, "A comparative study of in-sensor processing vs. raw data transmission using zigbee, ble and wi-fi for data intensive monitoring applications," in *Wireless Communications Systems (ISWCS), 2014 11th International Symposium on*. Ieee, 2014, pp. 519–524.

[47] (2018) Digi xbee. [Online]. Available: https://www.digi.com/pdf/ds-xbee-zigbee-mesh-kit.pdf

[48] (2018) Ts881. [Online]. Available: http://www.st.com/zh/amplifiers-and-comparators/ts881.html

[49] M. Q. Le, J.-F. Capsal, M. Lallart, Y. Hebrard, A. Van Der Ham, N. Reffe, L. Geynet, and P.-J. Cottinet, "Review on energy harvesting for structural health monitoring in aeronautical applications," *Progress in Aerospace Sciences*, vol. 79, pp. 147–157, 2015.

[50] J. Wang, R. Zhang, J. Yuan, and X. Du, "A 3-dimensional energy-harvesting-aware routing scheme for space nanosatellite networks," *IEEE Internet of Things Journal*, 2018.

[51] G. Zhao, H. Hu, S. Li, L. Liu, and K. Li, "Localization of impact on composite plates based on integrated wavelet transform and hybrid minimization algorithm," *Composite Structures*, vol. 176, pp. 234–243, 2017.